

## Electric-double-layer potential distribution in multiple-layer immiscible electrolytes: Effect of finite ion sizes

Siddhartha Das

*Physics of Fluids Group and J. M. Burgers Centre for Fluid Dynamics, University of Twente,  
P.O. Box 217, NL-7500 AE Enschede, The Netherlands*

(Received 27 September 2011; revised manuscript received 6 December 2011; published 17 January 2012)

In a recent study [S. Das and S. Hardt, *Phys. Rev. E* **84**, 022502 (2011).], we provided analytical results for the electric-double-layer (EDL) electrostatic potential distribution in a system of immiscible electrolyte layers confined between plates with gap dimensions comparable to the EDL thickness. We demonstrated that the intrinsic jumps in the ion-solvent interactions across the interface of the immiscible electrolytes lead to nontrivial electrostatic potential distributions that may completely defy or substantially augment the effect of the boundary wall potential. In this Brief Report, I extend this calculation to obtain analytical and numerical results for the case with finite ion sizes (or a finite ionic steric effect). It is found that the finite steric effect substantially enhances the contributions of jump in the ion-solvent interactions in the overall electrostatic potential distribution. More importantly, I demonstrate that such jumps in the ion-solvent interactions, owing to the immiscibility of the electrolytes, ensure that even for very weak wall zeta potentials, the steric effect can significantly affect the electrostatic potential distribution.

DOI: [10.1103/PhysRevE.85.012502](https://doi.org/10.1103/PhysRevE.85.012502)

PACS number(s): 82.45.Gj

The ionic and the electrostatic distribution adjacent to a charged wall, when an ionic aqueous solution comes in contact with that wall, is described by classical electric-double-layer (EDL) theory [1,2]. This theory is based on the solution of the Poisson-Boltzmann equation with the Poisson equation invoked to describe the EDL potential and the Boltzmann distribution for interrelating the ionic concentration to the EDL potential. However, the Boltzmann distribution is based on the mean field assumption, which considers the ions to be of point size. Over the years, there have been several attempts to modify this classical EDL theory by considering the finite sizes of the ions. (For a detailed review of the historical development of the EDL theories with finite ion size effects, refer to Refs. [3,4]). The finite ion size effect severely influences the different electrodynamic behaviors that have a remarkable impact on nanofluidic electrochemistry and transport [5–12]. One such potential problem, in which the effect of finite ion sizes has not yet been studied, is the estimation of the ionic distribution at the interface between two immiscible electrolytes. The classical solution for this problem is described by the formation of back-to-back electric double layers at the interface, first analyzed by Verwey-Niessen [13] invoking Gouy-Chapman theory [1,2,14]. Over the years, this simple description has been substantially elaborated to include factors like ion adsorption [15,16], molecular interactions [17], confinement effects [18], etc.

In this present Brief Report, I consider the effect of finite ion sizes on the EDL electrostatic potential distribution in a system of immiscible electrolytes with specified electrostatic potential at the domain boundaries. I consider the case in which the EDL thicknesses are comparable to the thicknesses of the electrolyte layers. Therefore, I am primarily extending the calculations provided in our previous paper [18] to highlight the consequence of considering finite ion sizes. I shall invoke a model proposed by Cervera *et al.* [19,20] to address the consequence of the finite ion size effect in EDL potential

distributions and appropriately modify it to include the contribution of finite ion-solvent interaction potential jumps that occur across the interface of the immiscible electrolyte layers. I first obtain closed-form analytical expressions for the case when there are two such electrolyte layers and extend it for the more general case of  $N$  layers. There are two principal results of this Brief Report. First is that the finite ion size considerations substantially enhance the consequences of jumps in the ion-solvent interaction potential; the alteration in the EDL distribution on account of such jumps is much more pronounced as compared to the case without the finite ion size effect [18]. Second, the finite ion-solvent interaction potentials ensure that even when the wall  $\zeta$  potential is significantly weak (i.e., one can employ a linearized Debye-Hückel treatment [14]), the steric effect can still influence the overall electrostatic potential. Classically, one needs to account for the finite ion size effect in case the wall potential has become large enough to excessively increase the counterion concentration [21]. The steric effect ensures a weakened crowding of the ions so that the wall potential shows a weaker decay, ensuring that at any point away from the wall, the magnitude of the potential is enhanced [21]. Therefore, it is universally believed (and demonstrated by Kilic *et al.* [21]) that a large wall potential is necessary for the non-negligible contribution of the steric effect in the overall potential. However, my present calculation demonstrates that in the presence of a suitable ion-solvent interaction potential jump, the potential can be substantially enhanced, thereby ensuring a non-negligible impact of the steric effect in the electrostatic potential even for a significantly small wall potential.

I consider a system of  $N$  layers of different immiscible electrolytes. (For a schematic of the problem corresponding to  $N = 2$ , refer to Fig. (1) of Ref. [18]). I start with the formulation of Cervera *et al.* [4,19,20], which considers the finite ion size effect in the electrostatic potential distribution and modify it to include the additional contribution for the

interaction of the ions with the solvent. Accordingly, for an ion of type  $i$ , I had

$$k_B T \ln(a_i) + ez_i \psi + \beta_i = \text{const}, \quad (1)$$

where

$$a_i = \frac{n_i/n_\infty}{1 - \nu \sum_k n_k/n_\infty}, \quad (2)$$

with  $\nu$  being the steric factor. Also in Eq. (1),  $n_i$  is the ion number density,  $n_\infty$  is the bulk value of the ion number density,  $k_B T$  is the thermal energy,  $e$  is the electronic charge,  $z_i$  is the ion valence (henceforth I shall use  $|z_i| = 1$ ),  $\psi$  is the electrostatic potential, and  $\beta_i$  is the ion-solvent interaction potential.

Equation (1) is applicable between any two points in the system. For example, consider two points: one in the bulk reservoir (where  $n_i = n_\infty$ ,  $\psi = 0$ , and  $\beta_i = 0$  so that  $a_i = \frac{1}{1-2\nu}$ ) and another in the nanochannel. Applying Eq. (1) between these two points, I can write

$$a_i = \frac{1}{1 - 2\nu} \exp \left[ -\frac{\text{sgn}(z_i) e \psi + \beta_i}{k_B T} \right]. \quad (3)$$

Equation (3) can be rearranged to obtain

$$\frac{n_+}{n_\infty} + \frac{n_-}{n_\infty} = \frac{g(\psi)}{1 - 2\nu + \nu g(\psi)}, \quad (4)$$

where

$$g(\psi) = \exp \left( \frac{-\beta_+ - e\psi}{k_B T} \right) + \exp \left( \frac{-\beta_- + e\psi}{k_B T} \right). \quad (5)$$

Hence, employing Eq. (2), we get

$$\frac{n_\pm}{n_\infty} = \frac{1}{1 - 2\nu + \nu g(\psi)} \exp \left( \frac{\mp e\psi - \beta_\pm}{k_B T} \right). \quad (6)$$

From the ionic concentration distributions, the electrostatic potential distribution is

$$\frac{d}{dy} \left[ \epsilon(y) \frac{d\psi}{dy} \right] = e(n_- - n_+), \quad (7)$$

where  $\epsilon$  is the permittivity. Equation (7) can be solved numerically to obtain the EDL electrostatic potential distribution [in the presence of the conditions expressed in Eqs. (9)–(11) as well as the boundary conditions expressed in Eq. (15)]. I can, however, further simplify the above equations applying Debye-Hückel linearization to  $\psi$  (valid for small  $\psi$ ) to obtain closed-form analytical expressions. The resulting modified Poisson-Boltzmann equation in a dimensionless form reads

$$\frac{d}{d\bar{y}} \left[ \bar{\epsilon}(\bar{y}) \frac{d\bar{\psi}}{d\bar{y}} \right] = \frac{h_1^2}{2\lambda^2} \frac{K_1 + K_2 \bar{\psi}}{K_3 + K_4 \bar{\psi}}, \quad (8)$$

where  $\bar{\psi} = e\psi/k_B T$ ,  $\bar{y} = y/h_1$  (here I consider two layers of immiscible electrolytes with the heights of the layers  $h_1$  and  $h_2$ , see Fig. (1) in Ref. [18] for the schematic),  $\bar{\epsilon} = \epsilon/\epsilon_w$  (where  $\epsilon_w$  is the permittivity of water), and  $\lambda = \sqrt{\epsilon_w k_B T / 2n_\infty e^2}$ . Also,  $K_1 = \exp(-\bar{\beta}_-) - \exp(-\bar{\beta}_+)$ ;  $K_2 = \exp(-\bar{\beta}_-) + \exp(-\bar{\beta}_+)$ ;  $K_3 = [1 - 2\nu + \nu \exp(-\bar{\beta}_-) + \nu \exp(-\bar{\beta}_+)]$ ; and  $K_4 = \nu [\exp(-\bar{\beta}_-) - \exp(-\bar{\beta}_+)]$ , where  $\bar{\beta}_i = \beta_i/k_B T$ .

As the system consists of two immiscible liquid layers, I can express the permittivity, the ionic interaction potential, and the steric factor as

$$\bar{\epsilon} = \bar{\epsilon}_1 \theta(1 - \bar{y}) + \bar{\epsilon}_2 \theta(\bar{y} - 1), \quad (9)$$

$$\bar{\beta}_\pm = \bar{\beta}_{1,\pm} \theta(1 - \bar{y}) + \bar{\beta}_{2,\pm} \theta(\bar{y} - 1), \quad (10)$$

$$\nu = \nu_1 \theta(1 - \bar{y}) + \nu_2 \theta(\bar{y} - 1), \quad (11)$$

where  $\theta(x)$  is the heaviside function.

Hence, denoting  $\bar{\psi}$  for  $0 \leq \bar{y} \leq 1$  as  $\bar{\psi}_1$  and  $\bar{\psi}$  for  $1 \leq \bar{y} \leq (1 + h_2/h_1)$  as  $\bar{\psi}_2$ , I can re-express Eq. (8) as

$$\bar{\epsilon}_1 \frac{d^2 \bar{\psi}_1}{d\bar{y}^2} = \frac{h_1^2}{\lambda^2} \frac{K_{1,1} + K_{2,1} \bar{\psi}}{K_{3,1} + K_{4,1} \bar{\psi}} \quad (\text{for } 0 \leq \bar{y} \leq 1) \quad (12)$$

and

$$\bar{\epsilon}_2 \frac{d^2 \bar{\psi}_2}{d\bar{y}^2} = \frac{h_1^2}{\lambda^2} \frac{K_{1,2} + K_{2,2} \bar{\psi}}{K_{3,2} + K_{4,2} \bar{\psi}} \quad \left( \text{for } 1 \leq \bar{y} \leq 1 + \frac{h_1}{h_2} \right), \quad (13)$$

where  $K_{1,1/2} = \exp(-\bar{\beta}_{1/2,-}) - \exp(-\bar{\beta}_{1/2,+})$ ,  $K_{2,1/2} = \exp(-\bar{\beta}_{1/2,-}) + \exp(-\bar{\beta}_{1/2,+})$ ,  $K_{3,1/2} = 1 - 2\nu_{1/2} + \nu_{1/2} \exp(-\bar{\beta}_{1/2,-}) + \nu_{1/2} \exp(-\bar{\beta}_{1/2,+})$ , and  $K_{4,1/2} = \nu_{1/2} [\exp(-\bar{\beta}_{1/2,-}) - \exp(-\bar{\beta}_{1/2,+})]$ .

To solve Eqs. (12) and (13), we simplify the expression in the right-hand side of the equations as follows:

$$\begin{aligned} & \frac{h_1^2}{\lambda^2} \frac{K_{1,1/2} + K_{2,1/2} \bar{\psi}}{K_{3,1/2} + K_{4,1/2} \bar{\psi}} \\ & \approx \frac{h_1^2 K_{1,1/2}}{\lambda^2 K_{3,1/2}} \left( 1 + \frac{K_{2,1/2}}{K_{1,1/2}} \bar{\psi} \right) \left( 1 - \frac{K_{4,1/2}}{K_{3,1/2}} \bar{\psi} \right) \\ & \approx \frac{h_1^2 K_{1,1/2}}{\lambda^2 K_{3,1/2}} \left[ 1 + \left( \frac{K_{2,1/2}}{K_{1,1/2}} - \frac{K_{4,1/2}}{K_{3,1/2}} \right) \bar{\psi} \right] \end{aligned} \quad (14)$$

with  $\frac{K_{4,1/2}}{K_{3,1/2}} \sim 1$  and  $\bar{\psi} \ll 1$  and dropping the term with  $\bar{\psi}^2$ . Employing Eq. (14) to simplify Eqs. (12) and (13), I can solve for the potential distribution analytically with the following boundary conditions:

$$\begin{aligned} (\bar{\psi}_1)_{\bar{y}=0} &= \bar{\zeta}_1, & (\bar{\psi}_1)_{\bar{y}=1} &= \bar{\psi}_c, \\ (\bar{\psi}_2)_{\bar{y}=1} &= \bar{\psi}_c, & (\bar{\psi}_2)_{\bar{y}=1+h_1/h_2} &= \bar{\zeta}_2, \end{aligned} \quad (15)$$

$$\left( \bar{\epsilon}_1 \frac{d\bar{\psi}_1}{d\bar{y}} \right)_{\bar{y}=1} = \left( \bar{\epsilon}_2 \frac{d\bar{\psi}_2}{d\bar{y}} \right)_{\bar{y}=1}.$$

Here,  $\bar{\psi}_c$  will be determined a posteriori.

The final analytical results are, accordingly,

$$\begin{aligned} \bar{\psi}_1 &= (A_1 + \bar{\psi}_c) \frac{\sinh \left( \frac{h_1}{\lambda_1^*} \bar{y} \right)}{\sinh \left( \frac{h_1}{\lambda_1^*} \right)} \\ &+ (A_1 + \bar{\zeta}_1) \frac{\sinh \left[ \frac{h_1}{\lambda_1^*} (1 - \bar{y}) \right]}{\sinh \left( \frac{h_1}{\lambda_1^*} \right)} - A_1, \end{aligned} \quad (16)$$

$$\begin{aligned} \bar{\psi}_2 &= (A_2 + \bar{\psi}_c) \frac{\sinh \left[ \frac{h_2}{\lambda_2^*} + \frac{h_1}{\lambda_2^*} (1 - \bar{y}) \right]}{\sinh \left( \frac{h_2}{\lambda_2^*} \right)} \\ &+ (A_2 + \bar{\zeta}_2) \frac{\sinh \left[ \frac{h_1}{\lambda_2^*} (\bar{y} - 1) \right]}{\sinh \left( \frac{h_2}{\lambda_2^*} \right)} - A_2, \end{aligned} \quad (17)$$

$$\bar{\psi}_c = \frac{\bar{\epsilon}_1 \left[ \frac{A_1 + \bar{\zeta}_1}{\sinh(h_1/\lambda_1^e)} - A_1 \coth(h_1/\lambda_1^e) \right]}{\bar{\epsilon}_1 \coth(h_1/\lambda_1^e) + \bar{\epsilon}_2 \frac{\lambda_1^e}{\lambda_2^e} \coth(h_2/\lambda_2^e)} + \frac{\bar{\epsilon}_2 \left[ \frac{A_2 + \bar{\zeta}_2}{\sinh(h_2/\lambda_2^e)} - A_2 \coth(h_2/\lambda_2^e) \right]}{\bar{\epsilon}_1 \frac{\lambda_2^e}{\lambda_1^e} \coth(h_1/\lambda_1^e) + \bar{\epsilon}_2 \coth(h_2/\lambda_2^e)}, \quad (18)$$

where

$$A_{1/2} = \frac{1}{\frac{K_{2,1/2}}{K_{1,1/2}} - \frac{K_{4,1/2}}{K_{3,1/2}}}, \quad \lambda_{1/2}^e = \lambda \sqrt{\frac{2\bar{\epsilon}_{1/2} K_{3,1/2}}{K_{1,1/2}}} \sqrt{A_{1/2}}. \quad (19)$$

The above results can be generalized for a system of  $N$  immiscible electrolyte layers as

$$\begin{aligned} \bar{\psi}_i &= (A_i + \bar{\psi}_{c,i-1/i}) \sinh\left(\frac{1}{\lambda_i^e} \sum_{k=1}^i h_k - \bar{y}\right) \\ &+ (A_i + \bar{\psi}_{c,i/i+1}) \sinh\left(\bar{y} - \frac{1}{\lambda_i^e} \sum_{k=1, i>1}^{i-1} h_k\right) \\ &- A_i \quad (\text{for } 1 \leq i \leq N), \end{aligned} \quad (20)$$

where  $\bar{\psi}_{c,i/j}$  is the potential at the interface between the adjacent layers  $i$  and  $j$ . Note that the known potentials at the bottom and the top boundaries are denoted as  $\bar{\psi}_{c,0/1}$  and  $\bar{\psi}_{c,N/N+1}$ , respectively, while the unknown interface potential is

$$\begin{aligned} \bar{\psi}_{c,i/i+1} &= \frac{\bar{\epsilon}_i \left[ \frac{A_i + \bar{\psi}_{c,i-1/i}}{\sinh(h_i/\lambda_i^e)} - A_i \coth(h_i/\lambda_i^e) \right]}{\bar{\epsilon}_i \coth(h_i/\lambda_i^e) + \bar{\epsilon}_{i+1} \frac{\lambda_i^e}{\lambda_{i+1}^e} \coth(h_{i+1}/\lambda_{i+1}^e)} \\ &+ \frac{\bar{\epsilon}_{i+1} \left[ \frac{A_{i+1} + \bar{\psi}_{c,i+1/i+2}}{\sinh(h_{i+1}/\lambda_{i+1}^e)} - A_{i+1} \coth(h_{i+1}/\lambda_{i+1}^e) \right]}{\bar{\epsilon}_i \frac{\lambda_{i+1}^e}{\lambda_i^e} \coth(h_i/\lambda_i^e) + \bar{\epsilon}_{i+1} \coth(h_{i+1}/\lambda_{i+1}^e)} \\ &\quad (\text{for } 1 \leq i \leq N-1), \end{aligned} \quad (21)$$

In Eqs. (20) and (21),

$$A_i = \frac{1}{\frac{K_{2,i}}{K_{1,i}} - \frac{K_{4,i}}{K_{3,i}}}, \quad \lambda_i^e = \lambda \sqrt{\frac{2\bar{\epsilon}_i K_{3,i}}{K_{1,i}}} \sqrt{A_i}. \quad (22)$$

It can be easily verified that by putting  $\nu = 0$  in Eqs. (16)–(22), I exactly recover the results of the previous paper [18] in which the finite ion size effect is not considered. Below, I discuss the results corresponding to  $N = 2$ ; however, the essential qualitative findings remain identical for any  $N$ .

Before explicitly highlighting the consequence of the finite steric effect on the EDL potential variation, I discuss what the analytical results predict at different limits. First consider  $\beta_{\pm} = 0$ . For such a case, in the presence of Debye-Hückel linearization on  $\psi$ , I can write [from Eq. (5)]  $g(\psi) = \exp(-e\psi/k_B T) + \exp(e\psi/k_B T) \approx 2$  such that  $n_{\pm}/n_{\infty} = \exp(\mp e\psi/k_B T) \approx 1 \mp e\psi/k_B T$ . Therefore, the EDL potential will be independent of the steric effect in absence of the ion-solvent interaction; this can be easily verified if one applies the Debye-Hückel linearization (valid for small wall potentials) to the equations governing the EDL potential distribution provided in Ref. [21]. Next consider the case  $\nu = 0$ . Analytical expressions for  $\bar{\psi}_{1,2}$  are identical to

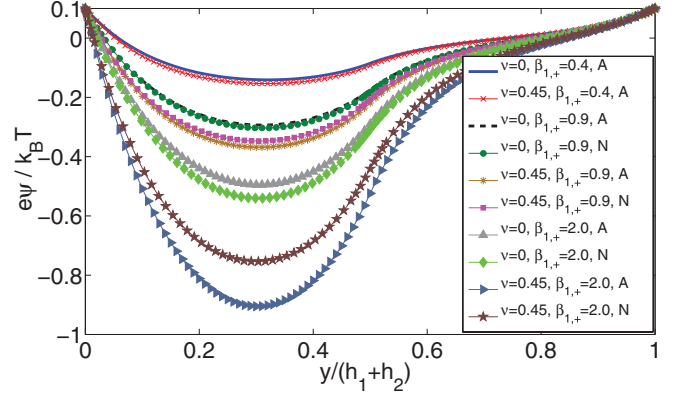


FIG. 1. (Color online) Variation of the EDL electrostatic potential for different values of the steric factor  $\nu$  (we always consider  $\nu_1 = \nu_2 = \nu$ ) and the ion-solvent interaction potential  $\beta_{1,+}$ . All other ion-solvent interaction potentials are zero. Other parameters are  $\epsilon_1/\epsilon_2 = 1$ ,  $h_1/h_2 = 1$ ,  $h_1/\lambda = 4$ , and  $\bar{\zeta}_1 = \bar{\zeta}_2 = 0.1$ . In the legend, “A” and “N” refer to the results corresponding to analytical and numerical solutions, respectively. Numerical results are obtained by solving the full nonlinear equation [Eq. (7)]. In the figure we do not show the numerical results corresponding to  $\beta_{1,+} = 0.4$  as they virtually coincide with those corresponding to the analytical results.

those obtained previously [18]. Also using the linearization for the expressions corresponding to the ion-solvent interactions (for reasons, see Ref. [18]), I can clearly see from Eq. (6) that if  $\beta_{+} = \beta_{-}$ ,  $n_{\pm}/n_{\infty} \approx 1 \mp e\psi/k_B T$ , i.e., the EDL potential will be independent of ion-solvent interaction energies. The other important issue is the appropriate choice of the ion-solvent interaction parameter  $\beta$ . We have proved in our previous paper [18] that only when  $\beta/(k_B T) < 1$  is it feasible to employ a Debye-Hückel linearized treatment as has been done for the present case. Hence, for all the analytical results that follow, I restrict myself to  $\beta_i/(k_B T) < 1$ .

In Fig. (1), I show the analytical and numerical results for the variation of the EDL potential as a function of the steric factor  $\nu$  and the ion-solvent interactions  $\beta_{1,+}$ . This figure conveys the two central findings of this Brief Report. It has been established [18] that the jump in the ion-solvent interaction potential for the coions (cations) leads to substantial lowering of the overall cation concentration ensuring a fast screening of the wall potential and large negative potential values (i.e., opposite in sign to the wall potential). Figure (1) clearly shows that the consideration of finite  $\nu$  augments this effect. The intrinsic lowering of the screening effect that can be associated with the consideration of finite ion sizes [21] ensures an even more pronounced screening of the wall potential and a larger negative electrostatic potential. Figure (1), therefore, clearly manifests that even for a substantially small wall  $\zeta$  potential, one can ensure a finite effect of the steric factor. This can be straightway attributed to the enhancement in the EDL potential due to the jump in the ion-solvent interaction potential. As an additional testament to this fact, one can witness [see Fig. (1)] a greater impact of the steric effect for larger  $\beta$  values. In summary, Fig. (1) in addition to clearly manifesting the enhancement in the overall potential induced

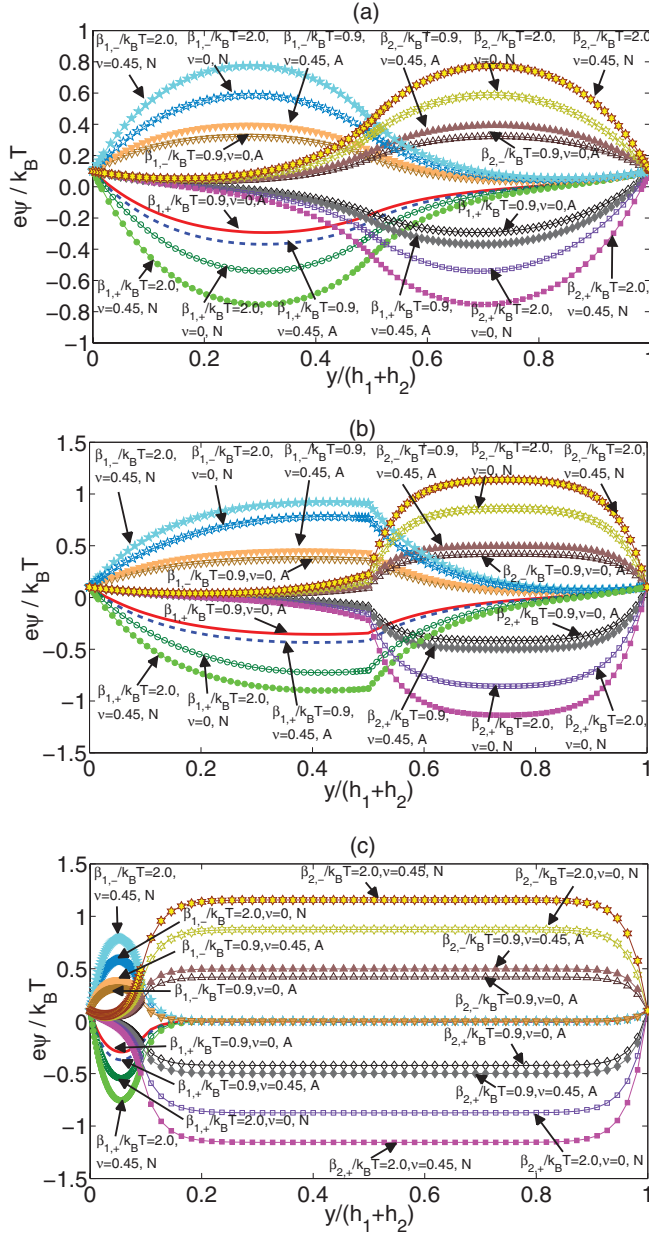


FIG. 2. (Color online) Variation of the EDL electrostatic potential for different values of the steric factor  $\nu$  (we always consider  $\nu_1 = \nu_2 = \nu$ ) and the ion-solvent interaction potential  $\beta_{1/2,\pm}$  for (a)  $\epsilon_1/\epsilon_2 = 1$  and  $h_1/h_2 = 1$ , (b)  $\epsilon_1/\epsilon_2 = 10$  and  $h_1/h_2 = 1$ , and (c)  $\epsilon_1/\epsilon_2 = 1$  and  $h_1/h_2 = 0.1$ . Other parameters are  $h_1/\lambda = 4$  and  $\zeta_1 = \zeta_2 = 0.1$ . In all these plots, only  $\beta_i$  has a finite nonzero value. Also, “A” and “N” refer to the results corresponding to analytical and numerical solutions, respectively. Numerical results are obtained by solving the full nonlinear equation [Eq. (7)].

by the finite steric effect also establishes that the ion-solvent interaction can be identified as an important factor which will ensure a non-negligible contribution of the steric effect even when the wall potential is very small; this clearly broadens the scope of the steric-effect-related problems wherein, so far, it has been universally accepted that non-negligible influences of the steric effect could be witnessed only for very large wall potentials [21]. We have previously demonstrated [18] that only when  $|\beta_i| < 1$  does the Debye-Hückel-based treatment produce acceptable results. For higher values of  $|\beta_i|$ , therefore, numerical solutions become unavoidable; for such values of  $|\beta_i|$ , one witnesses large differences in analytical and numerical results, clearly manifesting the invalidity of the analytical results for such  $|\beta_i|$  values. For example, in Fig. (1) for  $\nu = 0.45$ , the maximum deviation between the analytical and numerical results is 10% for  $\beta_{1,+} = 0.9$  and 22% for  $\beta_{1,+} = 2.0$ . Interestingly, for  $\nu = 0$ , numerical results predict a greater magnitude of the EDL potential whereas for  $\nu = 0.45$  this is reversed. Such an effect can be attributed to the lowering of the ionic number density gradient for finite  $\nu$  and larger  $\psi$  [manifested through the variation of the denominator on the right-hand side of Eq. (6)]. In the following results, I provide analytical results for  $\psi$  for  $|\beta_i| < 1$  (for such a case, the corresponding numerical results will provide some deviation) and numerical results for  $\psi$  for  $|\beta_i| > 1$  (for such a case, the analytical results will be completely invalid).

In Fig. (2), I demonstrate that for all kinds of  $\beta_i$  values, the steric effect magnifies the effect of the ion-solvent interaction. For all the cases, finite  $\beta_i$  leads to the depletion (or weaker screening) of the corresponding ions (i.e., cations for  $\beta_{i,+}$  and anions for  $\beta_{i,-}$ ). The finite steric effect enhances this weakening in screening, thereby leading to a more enhanced manifestation of the ion-solvent interaction potential jump in the overall electrostatic potential.

To summarize, I have demonstrated that the consideration of the finite steric effect can significantly enhance the impact of the ion-solvent interaction potential jump, witnessed at the interface between two immiscible electrolytes [18], in altering the EDL electrostatic potential distribution. Conversely, such a system of immiscible electrolytes, causing a jump in the ion-solvent interaction potential, can be viewed as a factor that ensures a non-negligible contribution of the steric effect even for a substantially small wall potential, thereby broadening the range of steric-effect-related studies that are primarily limited to cases with substantially large wall  $\zeta$  potentials [21].

The author gratefully acknowledges discussions with Prof. Steffen Hardt.

- [1] G. Gouy, *J. Phys.* **9**, 457 (1910).
- [2] D. L. Chapman, *Philos. Mag.* **25**, 475 (1913).
- [3] M. Z. Bazant, M. S. Kilic, B. D. Storey, and A. Ajdari, *Adv. Colloid Interface Sci.* **152**, 48 (2009).
- [4] S. Das and S. Chakraborty, *Phys. Rev. E* **84**, 012501 (2011).

- [5] A. Garai and S. Chakraborty, *Electrophoresis* **31**, 843 (2010).
- [6] C. K. Hua, I. S. Kang, K. H. Kang, and H. A. Stone, *Phys. Rev. E* **81**, 036314 (2010).
- [7] H. J. Zhao, *J. Phys. Chem. C* **114**, 8389 (2010).

- [8] A. S. Khair and T. M. Squires, *Q J. Fluid Mech.* **640**, 343 (2009).
- [9] B. D. Storey, L. R. Edwards, M. S. Kilic, and M. Z. Bazant, *Phys. Rev. E* **77**, 036317 (2008).
- [10] L. H. Olesen, M. Z. Bazant, and H. Bruus, *Phys. Rev. E* **82**, 011501 (2010).
- [11] M. Z. Bazant, M. S. Kilic, B. D. Storey, and A. Ajdari, *New J. Phys.* **11**, 075016 (2009).
- [12] M. Z. Bazant, B. D. Storey, and A. A. Kornyshev, *Phys. Rev. Lett.* **106**, 046102 (2011).
- [13] E. J. Verwey and K. F. Niessen, *Philos. Mag.* **28**, 435 (1939).
- [14] R. J. Hunter, *Zeta Potential in Colloid Science: Principles and Applications* (Academic, New York, 1981).
- [15] C. Gavach, P. Seta, and B. D'Epenoux, *J. Electroanal. Chem.* **83**, 225 (1977).
- [16] M. Gros, S. Gromb, and C. Gavach, *J. Electroanal. Chem.* **89**, 29 (1978).
- [17] I. Benjamin, *Annu. Rev. Phys. Chem.* **48**, 407 (1997).
- [18] S. Das and S. Hardt, *Phys. Rev. E* **84**, 022502 (2011).
- [19] J. Cervera, V. Garcia-Morales, and J. Pellicer, *J. Phys. Chem. B* **107**, 8300 (2003).
- [20] J. Cervera, P. Ramirez, J. A. Manzanare, and S. Mafe, *Microfluid. Nanofluid.* **9**, 41 (2010).
- [21] M. S. Kilic, M. Z. Bazant, and A. Ajdari, *Phys. Rev. E* **75**, 021502 (2007).